Applied Surface Science 314 (2014) 384–391

Contents lists available at ScienceDirect

Applied Surface Science

journal homepage: www.elsevier.com/locate/apsusc

Hydrogen photochromism in V_2O_5 layers prepared by the sol–gel technology

Yi Wang [a], Lei Pan [a], Yao Li [a,**], A.I. Gavrilyuk [b,*]

[a] Center for Composite Materials, Harbin Institute of Technology, China
[b] A.F. Ioffe Physical Technical Institute of the Russian Academy of Sciences, Sankt-Petersburg, Russia

ARTICLE INFO

Article history:
Received 7 May 2014
Received in revised form 18 June 2014
Accepted 26 June 2014
Available online 5 July 2014

Keywords:
Photochromism
Hydrogen diffusion
Photochemical reactions
V_2O_5

ABSTRACT

Here we report on hydrogen photochromism in V_2O_5 highly disordered layers, i.e., photochromism that occurs due to hydrogen atoms; the hydrogen being detached under the action of light from organic molecules adsorbed on the oxide surface, whereas the V_2O_5 layers have been prepared by the sol–gel technology. The comprehensive characterization of the layers has been carried out, as well as the investigation of the parameters influencing their photochromic sensitivity. The high photochromic sensitivity of the V_2O_5 layers is provided by the surface Grotthuss diffusion of the injected protons.

1. Introduction

The hydrogen photochromism in solids has its special niche, since it arises due to foreign species, namely hydrogen atoms, detached from hydrogen donor molecules under the action of light.

The detached hydrogen atoms can play the role either of dopant or catalyst, sometimes combining both functions, which can change dramatically parameters of solids or promote secondary processes.

The hydrogen-containing molecules (hydrogen donors), especially selected for this purpose, are adsorbed previously in dark on the surface of the transition metal oxides, such as WO_3, MoO_3, and V_2O_5 – famous multifunctional materials regarding hydrogen.

The mechanism of the photoinjection of hydrogen (PIH) into the oxides was described previously in detail [1,2]. A non-zero low-temperature reaction rate limit for photo-triggered hydrogen transfer between adsorbed molecules and the surface of highly disordered WO_3, MoO_3 and V_2O_5 films was discovered, and the reaction mechanism was determined as tunneling proton-coupled electron transfer [1,2].

The PIH has another important aspect since it is connected with production of atomic hydrogen under the action of light. This trend concerns energy processes; its investigation being important for fuel cells or for production of molecular hydrogen, since it may be expected to find an appropriate catalyst for transformation of atomic hydrogen H^0 into H_2 that is a fuel. The hydrogen photochromism can be also a useful tool in investigations of these processes being a crossing point for various contemporary scientific trends.

V_2O_5 is one of the transition metal oxides that are of great interest for researchers. First it is considered as a promising material for cathodes in lithium batteries [3–6]; it is very often used as a catalyst for various hydrogen abstraction reactions [7–10]; it can be also used as a material for chemical sensors [11–13]; it can be employed for degrading of hazardous organic substances [14]. Furthermore, V_2O_5 is investigated in electrochromism [15,16] and photochromism [2,17–20].

The V_2O_5 friable structure makes it possible to accommodate great quantities of hydrogen atoms, which leads to drastic changes in the oxide optical properties.

There are various methods of V_2O_5 film preparation, which yield different properties regarding the photochromism. Among these methods, sol–gel technology may be isolated. This method makes it possible to prepare facilely the layers of thickness ranging from tenths up to dozens of microns. A film of such thickness is very difficult to prepare by other conventional methods. Prior the hydrogen photochromism was investigated predominantly in evaporated V_2O_5 films [2,17–19], whereas it was poorly studied in V_2O_5 layers prepared by the sol–gel technology. To the best of our knowledge, there is only one paper concerning this issue [20], and it is clear that further comprehensive and detailed investigations are required.

* Corresponding author. Tel.: +7 812 5553497..
** Corresponding author.
E-mail addresses: yaoli@hit.edu.cn (Y. Li), gavrilyuk@mail.ioffe.ru (A.I. Gavrilyuk).

http://dx.doi.org/10.1016/j.apsusc.2014.06.167
0169-4332/

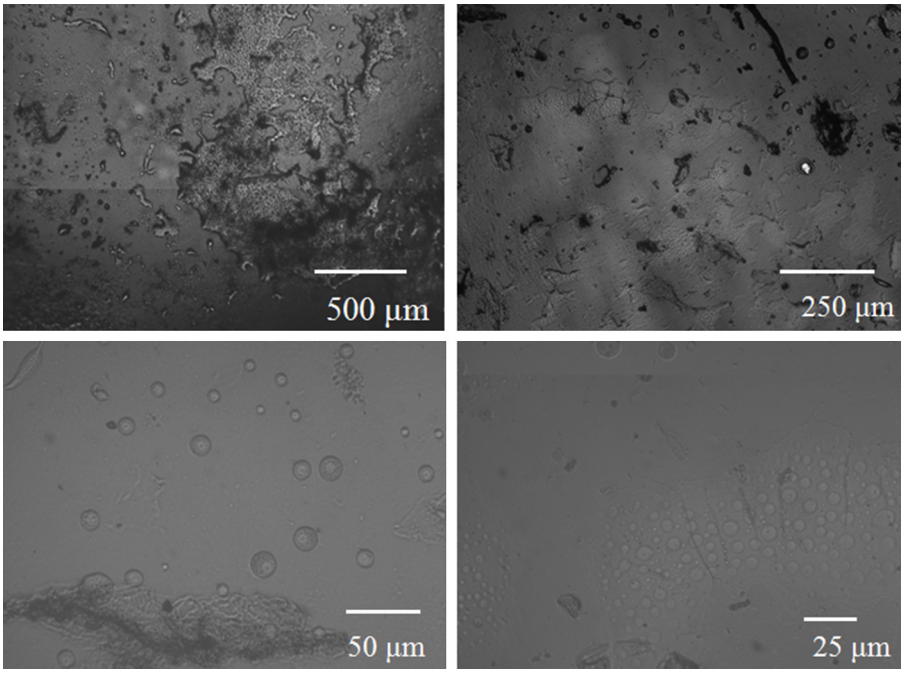

Fig. 1. Optical microscope images of the V_2O_5 gel surface under various magnifications (color on line). The scales are in micrometers.

The aim of this research was to fill the gaps in the investigations of the hydrogen photochromism in the V_2O_5 layers prepared by the sol–gel technology.

2. Preparation method

4 g of a 99% purity V_2O_5 powder was heated up to temperature of 850 °C and melted. The melt underwent splat cooling by pouring it into a vessel filled with 100 g of purified Aldrich water. This technology was used first already in 1911 [21]. After intensive stirring, the prepared sol was deposited onto glass substrates with the help of a pipette and dried for several hours at room temperature in air unless the sol turned into a xerogel. No additional heat treatment was employed since the aim was to prepare the xerogel with maximally developed and heterogeneous surface, which predetermines formation of highly reactive surface centers for the detachment of hydrogen atoms from the adsorbed molecules [1].

This technology gives a possibility to vary the film thickness in a wide range. In our experiments, the layer thickness was ranged between 0.35 μm up to 10 μm depending upon the sol mass deposited onto the substrates.

3. Layer characterization

3.1. Optical microscopy

Although sol–gel layers prepared by various techniques were characterized by many researchers [22–25], it makes sense to stress that namely this type of the V_2O_5 gels was not characterized properly. We provided a series of experiments with the aim to characterize completely the V_2O_5 xerogel properties with the help of various experimental facilities.

Several snapshots of the gel surface under various magnifications, made with the help of an optical microscope LW 300LJT (Shanghai Cewei Photoelectric Technology Co., Ltd.), show that the surface is highly heterogeneous (Fig. 1). One can observe numerous different non-homogeneities: cracks, bubbles, voids. Such a kind of morphology is determined by stochastic character of the drying process which predetermines existence of the domains with different properties.

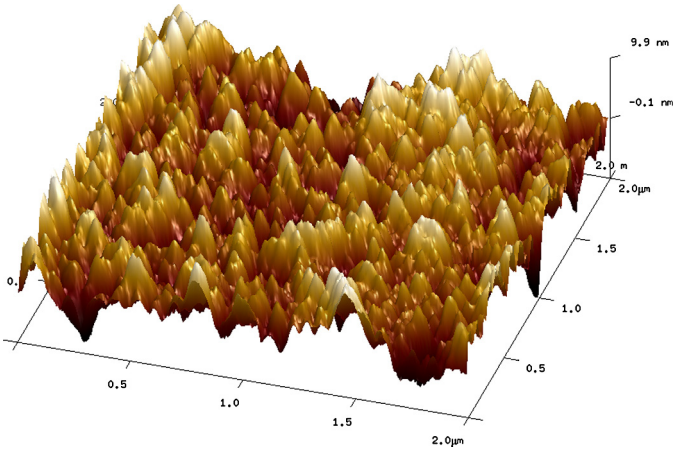

Fig. 2. The atomic force microscope image of the V_2O_5 the gel surface (color on line). The figures along the axes *X* and *Y* are in micrometers, whereas along the axe *Z* – in nanometers.

3.2. Atomic force microscopy

The atomic force microscope image of the gel surface made with the help of Bruker Fast Scan Dimension with Scan Asyst shows the gel morphology (Fig. 2) that confirms and complements the results obtained by the optical microscopy. One can see that the surface is highly heterogeneous and highly porous. The grains size ranges between 20 nm up to 50 nm in diameter. In some surface domains, these small grains are stacked in larger agglomerations of a poorly determined shape. All types of pores, namely, macro-, meso-, and micropores can be observed. The surface roughness is not high being within the limits between 10 and 15 nm. Thus, the pores are relatively non-deep. Various molecules (hydrogen donors) can be facilely accommodated into the surface pores.

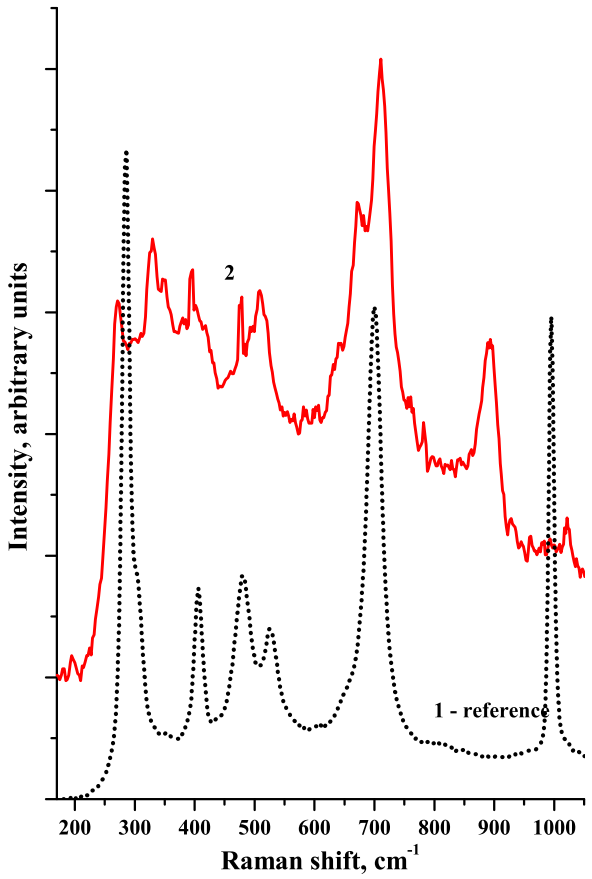

Fig. 3. Raman spectra for the V_2O_5 gel. 1 – for the powder, 2 – for the gel.

However, the surface morphology shows that the specific surface area for the V_2O_5 layers is much smaller as compared with that for the WO_3 and the MoO_3 films prepared by evaporation; see e.g. [1], which predetermines a smaller concentration of the surface reaction centers on the gel surface. For this reason, one would expect to have the photochromic sensitivity for the V_2O_5 gels essentially lower than that for the evaporated MoO_3 and WO_3 films.

3.3. Raman spectroscopy

The layer structure and composition were investigated also by Raman spectroscopy. We used an Ocean Optic Company spectrometer. The Raman spectra were taken in the quasi-backscattering geometry using 150 mW of the 785 nm line focused to a spot of 105 μm in diameter as the excitation source.

The Raman spectrum for the V_2O_5 layers and the reference spectrum for the V_2O_5 powder used for preparation of the layers are shown in Fig. 3, whereas the data concerning the Raman shift values are given in Table 1.

Prior V_2O_5 Raman spectra were investigated by numerous workers, and the Raman peaks are reliably assigned to the definite bond vibrations within the oxide structure, e.g. [26–32].

The structure of crystalline V_2O_5 is described as consisting of the packing of V_2O_5 layers along the *c* axis of the unit cell. To make the consideration more visual we present here the schemes illustrating the V_2O_5 structure.

Each layer is formed from VO_5 square pyramids (Fig. 4) sharing edges and corners (Fig. 5). Fig. 5 shows two cross sections of the V_2O_5 structure where possible positions for accommodation injected hydrogen atoms near different oxygen anions are depicted.

Table 1
Raman shift values for the V_2O_5 gel layers.

Powder Raman shift, cm^{-1}	Gel Raman shift, cm^{-1}
997	1021
	893
700	710
	671
527	509
481	479
406	394
	349
	330
286	271

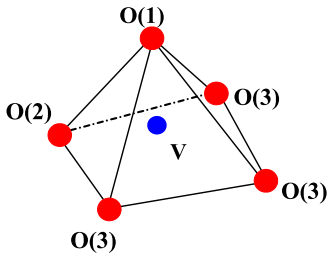

Fig. 4. The main structural unit of V_2O_5 – a square pyramid.

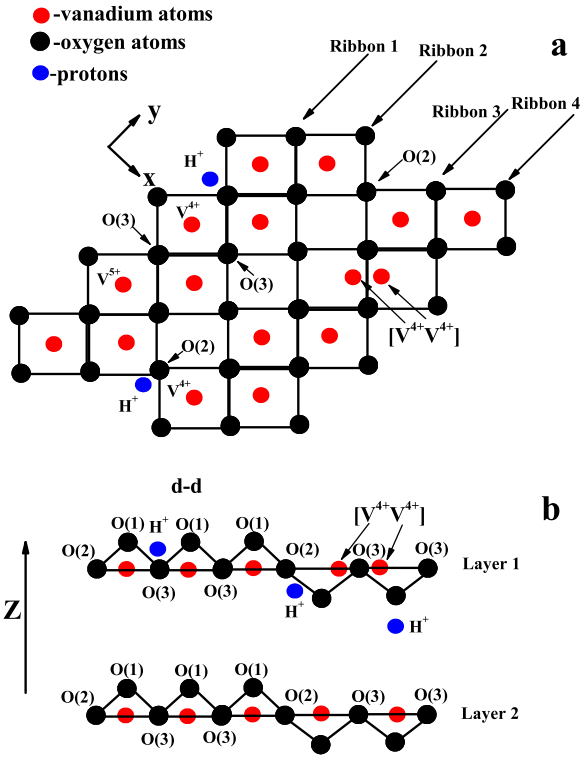

Fig. 5. The scheme of the layered V_2O_5 structure where possible positions for the inserted hydrogen atoms are depicted.

The pyramids sharing only corners form a ribbon; two of these ribbons inserted one into the other form a row. The double-ribbon rows form sheets by sharing corners with the other similar ribbon-rows on both sides. All pyramids in one row point up and the ones in the neighboring rows point down (Fig. 5). The sheets form a three-dimensional network being stacked one over the other so that apices of the pyramids of one sheet are positioned over V atoms located in the centers of the basal planes of pyramids of the sheets

beneath, thus completing the distorted octahedron. V_2O_5 structure exhibits layers consisting of zigzag rows of vanadium-oxygen pyramids (Fig. 5).

Within the VO_5 pyramid, a very short V=O double bond (1.54 Å) is observed, while between adjacent V_2O_5 layers the V—O bonds are very long (2.81 Å), which lead the two-dimensional character of V_2O_5 [29]. The high-frequency Raman peak at about 997 cm^{-1} (Fig. 3, curve 1 and column 1 of the table) corresponds to the V_1=O stretching mode [29]. The peak at 700 cm^{-1} is assigned to the —V—O—V— stretching vibration, which results from corner-shared oxygens common to two pyramids [30]. The peak located at 527 cm^{-1} is assigned to the V_3—O) stretching mode which results from edged-shared oxygens in common to three pyramids [30,31]. The two peaks located at 406 and 286 cm^{-1} are assigned to the bending vibration of the V=O bonds [30]. The peaks located at 487 and 303 cm^{-1} are assigned to the bending vibrations of the bridging V—O—V (doubly coordinated oxygen), and the triply coordinated oxygen (V_3—O) bonds, respectively [30].

The Raman spectrum of the V_2O_5 layers (Fig. 3, curve 2) exhibits a pronounced difference as compared with that of the V_2O_5 powder (curve 1). Several peaks are noticeably shifted: the peak at 997 cm^{-1} is shifted to 1021 cm^{-1}, the peak at 700 cm^{-1} is shifted to 710 cm^{-1}, the peak at 527 cm^{-1} is shifted to 509 cm^{-1}, the peak at 406 cm^{-1} is shifted to 394 cm^{-1}, and the peak at 286 cm^{-1} is shifted to 271 cm^{-1}. Furthermore a series of additional peaks was observed that do not belong to the V_2O_5 at 893, 671, 349, and 330 cm^{-1}. According to [33] the presence of relatively strong bands existing at 504 cm^{-1} and 682 cm^{-1} could indicate the mixed valence oxide V_4O_9 described by the formula $V_2^{4+}V_2^{5+}O_9^{2-}$ [34]. These values are very close to those at 509 cm^{-1} and 671 cm^{-1} observed in this research. In favor of this assignment is also that the band at 1032 cm^{-1} which was detected in V_4O_9 films [34]. Thus, we can make the conclusion that the V_2O_5 gels comprise several vanadium oxide phases.

Since the layers were prepared from the melt, they have some oxygen deficiency which leads to the appearance of the lower valency V^{4+} cations (reduction of the oxide); the oxygen vacancies being formed by the powder heat treatment and due to the chemical reaction between the melt and water.

The oxygen vacancies may be randomly distributed within the sol. The drying process is carried out under highly non-equilibrium conditions and at room temperature, which doesn't allow forming of an ordered oxide structure: only metastable precipitates of the oxide phases can be generated. Similar phenomenon was observed earlier by the anodic oxidation of vanadium [33], where these metastable phases arisen due to high degree of the surface disorder were observed by the Raman spectroscopy.

3.4. IR-FTIR spectroscopy

Fig. 6 shows the IR-FTIR spectra for the xerogels scraped from the substrates and mixed with a KBr powder. After that a tablet was pressed that was used for the FTIR measurements. There are three peaks belonging to the stretching vanadium-oxygen vibrations: at 1005 cm^{-1} attributed to V=O stretching vibration of the terminal oxygen (vanadyl), the second peak at 760 cm^{-1} is assigned to the doubly coordinated oxygen (V_2—O) stretching mode, that is —V—O—V— stretching vibration, which results from corner-shared oxygens common to two pyramids, the third peak at 520 cm^{-1} is assigned to the triply coordinated oxygen (V_3—O) stretching mode which results from edged-shared oxygens in common to three pyramids [35].

Other peaks don't belong to the vanadium pentoxide. The peak at ν = 3420 cm^{-1} may be unambiguously assigned to the O–H stretching vibration of the OH bonds in water molecules, whereas the peak at ν = 1620 cm^{-1} is attributed to the bending H–O–H

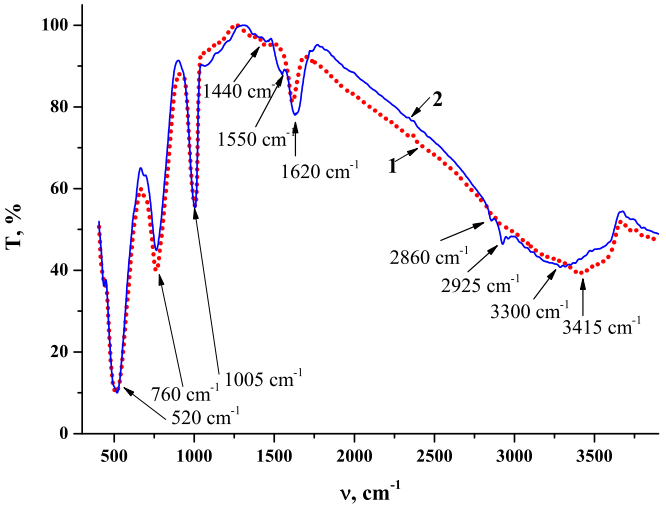

Fig. 6. Transmission IR spectra for the vanadium oxide xerogels: (1) before illumination; (2) after 5 h of the illumination.

vibration. The presence of the large amount of water inside of the xerogel structure is very important since proton diffusion is facilitated along the net of hydrogen bonds formed by water molecules according to the Grotthuss mechanism of the diffusion [36–38]. We return back to this figure when we discuss the photochromic properties of the V_2O_5 gel layers.

4. Photochromism in the V_2O_5 layers

The V_2O_5 layers were illuminated by a filtered light of a 250 W power high-pressure mercury lamp (Shanghai Yayuan Lighting Appliance Co. Ltd.). The irradiation bands in the UV range were cut off by a filter except the band peaked at 365 nm (E = 3.4 eV) that was used for generation of electron–hole pairs. The distance between the lamp and the sample surface was 23 cm. The specific power of the photons falling on the oxide surface was ~20 mW cm^{-2}. The sample temperature didn't exceed 25 °C under the illumination which was carried out on air in ethanol vapor. The sample was placed into the cylindrical cell of 35 mm height and of 55 mm diameter with a 40-mm-thick quartz window. Another small cylindrical vessel filled with ethanol was put inside of the cell to provide the saturated ethanol vapor pressure.

The layer thickness d was calculated using the reflection spectra (see the supplementary materials) where the interference fringes are well resolved.

The formula (1) was used:

$$d = \frac{1}{(1/\lambda_n - 1/\lambda_{n-1})2n} \quad (1)$$

where λ_n and λ_{n-1} are the wavelengths of two adjacent extremes in the interference fringes. We selected the lowest-energy extremes where the refractive index dispersion is negligible. The refractive index value was taken n = 1.9 [39].

No photochromism was observed if the illumination by photons of energy higher than the V_2O_5 band gap, that is E_g = 2.2–2.4 eV (see [15] and refs therein), was carried out in air or under vacuum. The situation radically changed when the special hydrogen donor molecules were adsorbed on the layer surface.

Fig. 7 presents an example of the optical density D spectra before and after illumination. The broad absorption band peaked at E = 0.8 eV (in the near IR range) and covering the entire visible range grew continuously under the illumination (curves 2–4, Fig. 7), which is the reason for the color changes (photochromism) in the layer. This intensive optical absorption band has a non-Gaussian

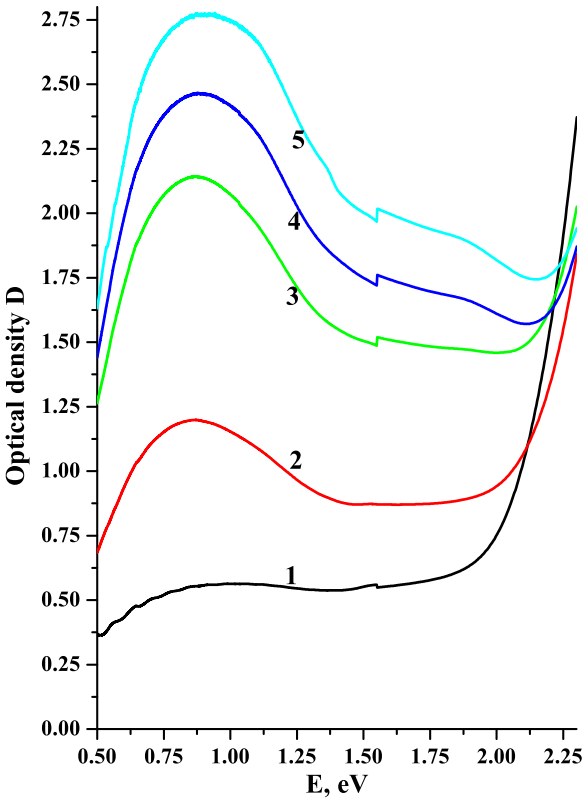

Fig. 7. Optical density D spectra of the V_2O_5 layers before and after illumination: (1) before illumination; (2) after illumination, illumination time t = 10 min; (3) t = 30 min; (4) t = 60 min; (5) t = 120 min. Film thickness d = 4.2 μm.

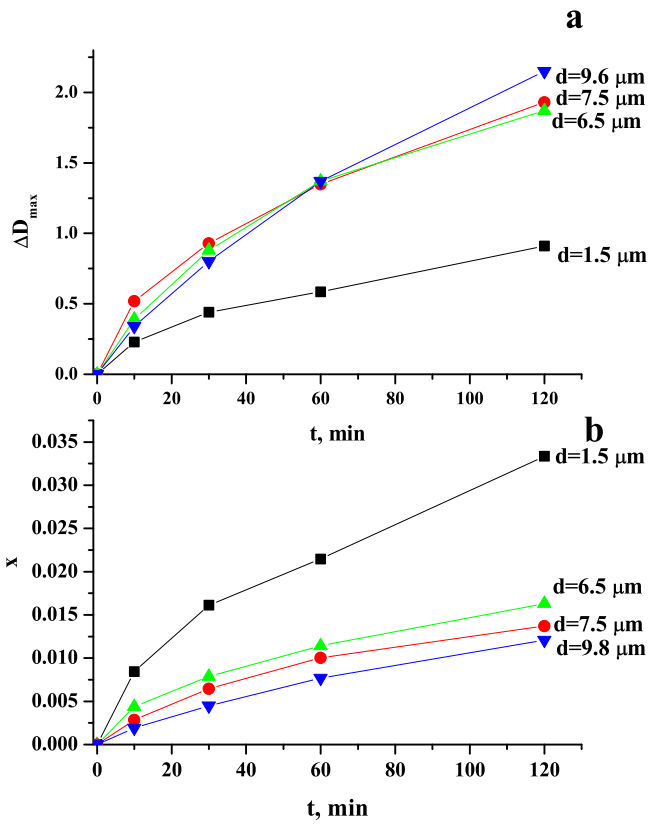

Fig. 8. Photoinduced optical density ΔD_{max} at the band maximum (a) and concentration of inserted hydrogen atoms x (b) versus illumination time t for the films of various thickness.

shape (Fig. 7), which implies that the absorption bell is comprised of several bands belonging to different absorption centers. Due to the non-uniform broadening in the highly disordered structure, the peaks belonging to the different bands are not resolved except the band peaked at E = 0.8 eV. In favor of this hypothesis, it could be said that several absorption bands were resolved in the nanosized WO_3 and MoO_3 films having a very high specific surface area [40]. It is worthwhile to notice that the position of the arising absorption band in the spectral range is very different to that in the evaporated highly disordered V_2O_5 films [2], which implies also that different centers arise under the illumination in the both V_2O_5 films.

One can notice (Fig. 7, curve 1) that the same optical absorption band, although of much lower intensity, is present in the xerogel before the illumination, which shows the presence of the V^{4+} lower-valency cations. The reasons for that can be both oxygen deficiency formed by the powder heat treatment and the reduction of the melt due to reaction with water. Due to the splat cooling some hydrogen atoms can be injected into the V_2O_5 colloids. It is well known that the nature of the optical absorption band is the optical transition between neighboring non-isovalent cations V^{4+} and V^{5+}, see [15] and refs therein:

$$V^{4+}(A) + V^{5+}(B) + h\nu \rightarrow V^{5+}(A) + V^{4+}(B).$$

The reverse electron transition is also possible, which can return the system into the initial situation. The optical transitions between non-isovalent cations under the action of light yield the exchange of the valency for neighboring cations.

The kinetics of the PIH can be illustrated by Fig. 8a, where the characteristic curves are presented, that is the dependences of the photoinduced optical density ΔD_{max} in the band maximum versus illumination time t.

For further consideration it is important to demonstrate how the concentration N of the injected hydrogen atoms (color centers) changes under the illumination.

The concentration N (cm^{-3}) of the centers inserted into a WO_3 film can be roughly estimated from Smakula's equation [41]:

$$N \times f = 0.87 \times 10^{17} \frac{n}{(n^2+2)^2} \alpha_{max} W \quad (2)$$

where f is the oscillator strength, n is the refractive index, α_{max} is the absorption coefficient in the band maximum (in cm^{-1}) and W is the half-bandwidth (in eV). If the reflection losses are neglected, then:

$$\alpha_{max} \approx 2.31 \frac{D_{max}}{d} \quad (3)$$

where d is film thickness.

Then with the measured values of D_{max}, taken from Fig. 8a, $W \approx 1$ eV, and refractive index n = 1.9 [39], using Smakula's equation [41] one gets the values of the concentration of inserted hydrogen atoms N. With the values of the V_2O_5 density of 3.36 g cm^{-3} and the molecular mass 182 g mol^{-1} we get the concentration of V_2O_5 units $N_{V_2O_5} = 1.1 \times 10^{22}$ cm^{-3}. Then it is easy to estimate the value of x that is the ratio between the concentration of the hydrogen atoms and the concentration of the vanadium atoms in the formula $H_xVO_{2.5}$.

$$x = \frac{N}{N_{V_2O_5}} \quad (4)$$

We investigated the hydrogen photochromism in the layers of different thickness and found that both the photochromic sensitivity (PS) and the shape of the arising absorption band depend upon the film thickness. This is an interesting finding which makes sense

to discuss. The PS of the samples was determined by the characteristic curve, i.e., by the dependence of the optical density ΔD_{max} in the band maximum against illumination time t.

The example of the dependences of the optical density ΔD_{max} in the band maximum and the value of x upon film thickness versus illumination time t are presented in Fig. 8a and b. As it is seen in Fig. 8a, the maximal PS is achieved in the very thick layers dropping down to a very small value in the thin xerogels.

It is worthwhile to emphasize the paradoxical situation here: although the higher photochromic sensitivity is achieved in the thicker films, the higher concentration of the injected hydrogen centers is achieved in the thinner ones (see Fig. 8a and b). Meanwhile x in these films reaches the value much less than that in H_xWO_3 and H_xMoO_3 photochromic films [1] and in $H_xV_2O_5$ films evaporated directly in hydrogen donor vapor, where the value of x is an order of the magnitude higher [2]. The low value of x explains also the relatively small "blue" shift of the fundamental absorption edge (see Fig. 7), which is observed usually by the photochromism or electrochromism in V_2O_5 films [15]. It was previously shown that this shift can reach the value of ≈1 eV in the evaporated V_2O_5 films if the x value reaches 0.6–0.8 [2]. In our case this value is much lower, which explains in turn the much lower value for the shift of the fundamental absorption edge.

It is clear that the relatively high PS in these layers is achieved due to their high thickness. Physically it means that the diffusion of the electron-proton plasma is the factor that makes it possible to achieve the high PS. It was already shown that the efficiency of the hydrogen photochromism drops down with the increase of the Fermi level position that always takes place when electron-proton plasma is injected into oxide [42]. The diffusion of this plasma into the film depth reduces the concentration of the injected centers (they disperse over bigger volume) which in turn lowers the Fermi level position. The diffusion of the electron-proton plasma depends upon the slowest particle that is upon a proton. The films obtained with the help of the sol–gel technology contain a big amount of the adsorbed water which can serve as specific channels where diffusion is facilitated due to the Grotthuss mechanism (see Fig. 6). Just for this reason enhancement of the layer thickness yields the enhancement of the film PS.

We can roughly estimate the value of the electron-proton plasma diffusion coefficient in the direction perpendicular to the film surface. If we insert the values of 7.5 μm and 9.6 μm (see Fig. 8a) for the 120 min exposure into the formula:

$$D = \frac{l^2}{4t}, \tag{5}$$

where l is the distance passed by a particle, t is the diffusion time.

We get the value of the diffusion coefficient $D \geq 2 \times 10^{-11}$ cm^2/s in the direction perpendicular to the layer surface.

These values are higher than those reported for the WO_3 highly disordered films [42], and that is the reason why the thick V_2O_5 gel layers demonstrate the PS that is comparable with that of the WO_3 and the MoO_3 films mentioned. The V_2O_5 layers have much smaller specific surface area and, due to this, much smaller concentration of the reaction centers, but this loss in the sensitivity is compensated by the higher proton diffusions coefficient. For this reason it is possible to achieve relatively high PS in the thick V_2O_5 layers.

Another interesting finding is that the absorption band drastically widens in the high energy part of the spectral range with the concentration of the inserted hydrogen atoms x (Fig. 9).

The reason for this drastic widening could be formation of the different centers which arise in the layer due to hydrogen atoms [40]. As it was already shown, different centers can arise by the PIH. The hydrogen atoms being detached from the hydrogen containing molecules can diffuse into the film depth into the domains which are not illuminated by the light. Due to the high absorption

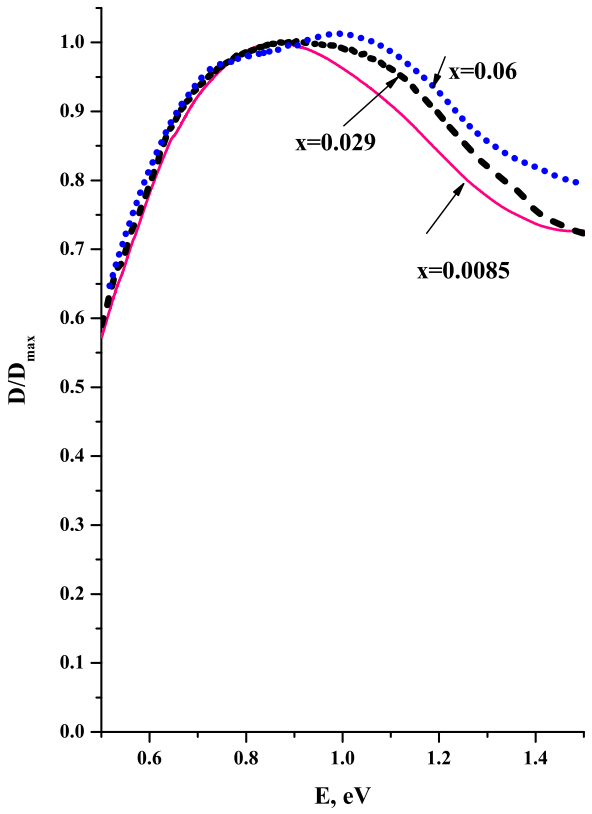

Fig. 9. Normalized bands D/D_{max} for the V_2O_5 films.

coefficient in the range of the fundamental absorption edge the light penetrates into the film in the depth approximately 1–1.5 μm. For thin films, the energy delivering by the light can provide formation of the paired diamagnetic centers. Formation of the different types of the centers yields the changes in the absorption band [2]. It was shown that at the concentrations of the injected centers is 0.6–0.8 in the formula $H_xVO_{2.5}$ [2], the absorption band is very different to that shown in Fig. 7. High concentration of the injected centers leads to pairing and formation of diamagnetic centers especially when the diffusion is hampered [40].

However, the fact that the concentration of the injected center is much higher in the thin films than in the thick ones shows that definite number of the reaction centers is lost during the illumination. It might be caused either by the formation of oxygen vacancies or by the blockade of the centers due to chemisorption of water molecules. We return back to Fig. 6 that shows the chemisorption of water really takes place under the action of light. It is easy to notice that after the illuminations of the layer the peak attributed to the O–H stretching vibrations is shifted from $\nu = 3420\,cm^{-1}$ to $\nu = 3290\,cm^{-1}$ which proves the change of the water state under illumination. This effect is similar to that in quasi-amorphous WO_3 and MoO_3 films and is attributed to the transition of water molecules from the physical adsorption to the chemisorptions [15].

Furthermore the three new peaks arise in the spectra after the illumination, which is attributed to residual of ethanol used as a hydrogen donor: the duplet at 2925 and 2865 cm^{-1} that is assigned to the asymmetric and symmetric CH_3 vibrations, correspondingly, in ethanol, and the peak at 1545 cm^{-1} attributed to the bending vibrations of these group (Fig. 6). The information concerning the residuals of ethanol can give some prompts and hints regarding the hydrogen transfer mechanism. It should be underlined that the PIH doesn't yield essential changes in the IR spectrum in the range of the V–O vibrations, since the concentration of the inserted center is

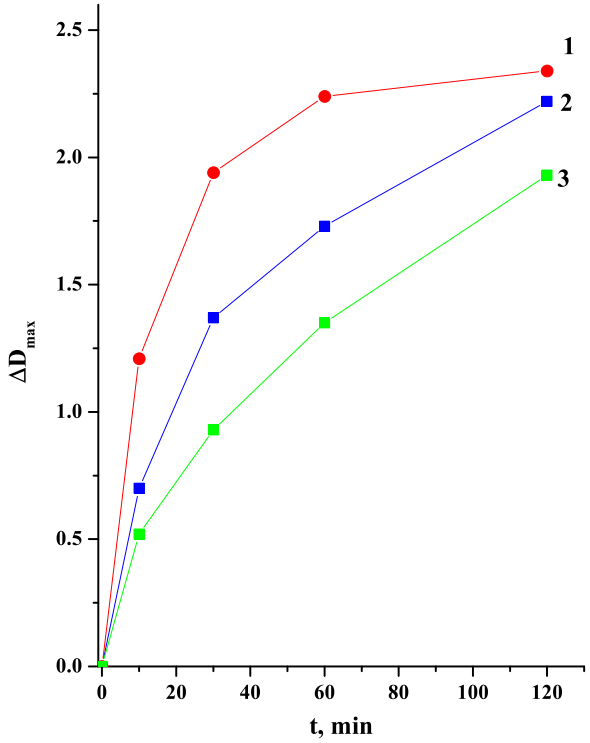

Fig. 10. The changes of the photochromic sensitivity of the layers after storage of the sol in air. 1 – For the as prepared sol, 2 – after 1 month storage of the sol in a refrigerator at $T = 5\,^{\circ}C$, 3 – after 1 month storage of the sol at $T = 20\,^{\circ}C$. Film thickness $d = 7.5\,\mu m$.

not high. For the same reason the Raman spectra also demonstrate insignificant changes under the illumination.

The chemisorption which can also take place in dark is the reason of the film aging that is the loss of the PS during storage. This aging concerns both the sol and the gel; a typical example for the sols being presented in Fig. 10. It comes out as a decay of the photochromic sensitivity of the layers after storage of the sols or the prepared gels under normal conditions. The storage of the sols at lower temperature (in refrigerator) retards this aging but it does not eliminate it (Fig. 10). For this reason we used to work with as prepared samples. The IR spectroscopy measurements showed that the changes in the spectra for the bands belonging to the vibrations of water molecules adsorbed on the oxide surface are the same as those under illumination, which makes it possible to attribute the aging to the chemisorptions of water which blockades of the reaction centers.

5. Conclusions

1. We characterized the gel layers prepared by splat cooling of V_2O_5 melt using various experimental facilities. It was shown that the layers obtained are highly heterogeneous and consist of several metastable oxide phases.
2. These layers contain a great amount of the adsorbed water and exhibit good photochromic properties.
3. We investigated the hydrogen photochromism using the layers of different thickness and found that both the photochromic sensitivity and the shape of the arising absorption band depend upon the film thickness. The maximum photochromic sensitivity is achieved in the very thick layers dropping down to a very small value in the thin xerogels. The proton diffusion makes it possible to achieve the high photochromic sensitivity even at relatively low concentrations of the injected hydrogen atoms. At the same time the absorption band drastically widens in the high energy part on decrease of the layer thickness.

   The reason for this drastic widening could be formation of different centers which arise in the layer with hydrogen atoms. As it was already shown, different centers can arise by the photoinjection of hydrogen. The hydrogen atoms being detached from the hydrogen containing molecules can diffuse into the film depth into the domains which are not illuminated by the light. Due to the high absorption coefficient in the range of the fundamental absorption edge the light penetrates into the film in the depth approximately 1–1.5 μm. For thin films the energy delivering by the light can provide formation of the paired diamagnetic centers. Formation of the different types of the centers yields the changes in the absorption band structure.
4. We showed that the V_2O_5 layers obtained with the help of splat cooling of V_2O_5 melt are perspective materials for the investigations of the hydrogen photochromism. We are going proceed further with this research and provide other facilities, e.g. ESR, that makes it possible to go deeper in the understanding of the process. We will also be concentrated on the technological experiments aiming to enhance the specific surface area of the V_2O_5 layers.

Acknowledgments

We thank National Natural Science Foundation of China (No. 51010005, 90916020, 51174063), Natural Science Funds for Distinguished Young Scholar of Heilongjiang province, and the project of International Cooperation supported by Ministry of Science and Technology of the People's Republic of China (2013DFR10630).

The research was carried out within the frames of the cooperation agreement in scientific research between the Harbin University of Technology and A.F. Ioffe Physical Technical Institute.

Appendix A. Supplementary data

Supplementary data associated with this article can be found, in the online version, at http://dx.doi.org/10.1016/j.apsusc.2014.06.167.

References

[1] A. Gavrilyuk, U. Tritthart, W. Gey, Photo-stimulated proton-coupled electron transfer in quasi-amorphous WO_3 and MoO_3 thin films, Phil. Mag. 87 (2007) 4519–4553.
[2] A. Gavrilyuk, U. Tritthart, W. Gey, Photoinjection of hydrogen and the nature of a giant shift of the fundamental absorption edge in highly disordered V_2O_5 films, Phys. Chem. Chem. Phys. 13 (2011) 9490–9497.
[3] P. Poizot, S. Laruelle, S. Grugeon, L. Dupont, J.-M. Tarascon, Nano-sized transition-metal oxides as negative-electrode materials for lithium-ion batteries, Nature 407 (2000) 496–499.
[4] C.R. Walk, N. Margalit, δ-LiV_2O_5 as a positive electrode material for lithium-ion cells, J. Power Sources 68 (1997) 723–725.
[5] C.V. Ramana, R.J. Smith, O.M. Hussain, M. Massot, C.M. Julien, Surface analysis of pulsed laser-deposited V_2O_5 thin films and their lithium intercalated products studied by Raman spectroscopy, Surf. Interface Anal. 37 (2005) 406–411.
[6] G.P. Holland, J.L. Yarger, D.A. Buttry, F. Huguenin, R.M.J. Torresi, Solid state NMR study of ion-exchange process in V_2O_5 xerogel, polyaniline/V_2O_5, and sulfonated polyaniline/V_2O_5 nanocomposites, J. Electrochem. Soc. 150 (2003) A1718–A1722.
[7] H. Launay, S. Loridant, A. Pigamo, J.L. Dubois, J.M.M. Millet, Vanadium species in new catalysts for the selective oxidation of methane to formaldehyde: specificity and molecular structure dynamics with water, J. Catal. 246 (2007) 390–398.
[8] B.M. Weckhuysen, D.E. Keller, Chemistry, spectroscopy and the role of supported vanadium oxides in heterogeneous catalysis, Catal. Today 78 (2003) 25–46.
[9] J. Łojewska, B. Źrałka, W. Makowski, R. Dziembaj, Promoting methane partial oxidation: homogenous additives impact on formaldehyde yield on vanadia catalyst, Catal. Today 101 (2005) 73–80.
[10] Ch. Zhao, I.E. Wachs, Selective oxidation of propylene to acrolein over supported V_2O_5/Nb_2O_5 catalysts: an in situ Raman, IR, TPSR and kinetic study, Catal. Today 118 (2006) 332–343.

[11] R. Rella, P. Siciliano, A. Cricenti, R. Generosi, M. Girasole, L. Vanzetti, M. Anderle, C. Coluzza, A study of physical properties and gas-surface interaction of vanadium oxide thin films, Thin Solid Films 349 (1999) 254–259.
[12] M. Caldararu, C. Munteanu, P. Chesler, M. Carata, C. Hornoiu, N.I. Ionescu, G. Postole, V. Bratan, Supported oxides as combustion catalysts and as humidity sensors. Tuning the surface behavior by inter-phase charge transfer, Microporous Mesoporous Mater. 99 (2007) 126–131.
[13] W. Fergus, Materials for high temperature electrochemical NO_x gas sensors, Sens. Actuators 121 (2007) 652–663.
[14] J.-H. Li, H.-W. Ma, W.-H. Huang, Effect of V_2O_5 on the properties of mullite ceramics synthesized from high-aluminum fly ash and bauxite, J. Hazard. Mater. 166 (2009) 1535–1539.
[15] C.G. Granqvist, Handbook of Inorganic Electrochromic Materials, Elsevier, Amsterdam–Lausanne–New York–Oxford–Shannon–Tokyo, 1995.
[16] A. Talledo, C.G. Granqvist, Electrochromic vanadium-pentoxide-based films: structural electrochemical, and optical properties, J. Appl. Phys. 77 (1995) 4655–4666.
[17] A.I. Gavrilyuk, N.M. Reinov, F.A. Chudnovskii, Photo- and thermochromism in V_2O_5 films, Sov. Tech. Phys. Lett. 5 (1979) 514–515.
[18] A.I. Gavrilyuk, A.A. Mansurov, F.A. Chudnovskii, Photoinjection of hydrogen in amorphous MoO_3 and V_2O_5 films, Sov. Tech. Phys. Lett. 10 (1984) 292–293.
[19] A. Gavrilyuk, Nature of photochromism in amorphous V_2O_5 thin films. Optical, organic, and semiconductor inorganic materials, Proc. SPIE 2968 (1997) 195–200.
[20] A.I. Gavrilyuk, T.G. Lanskaya, Photochromism in thin V_2O_5 layers prepared by the sol-gel technology, Tech. Phys. Lett. 20 (1994) 219–221.
[21] C. Sanchez, P. Babonneau, R. Marineau, J. Livage, J. Bullot, Semiconducting properties of V_2O_5 gels, Phil. Mag. 47 (1983) 279–290.
[22] J. Livage, Vanadium pentoxide gels, Chem. Mater. 3 (1991) 578–593.
[23] O. Pelletier, P. Davidson, C. Bourgaux, C. Coulon, S. Regnault, J. Livage, A detailed study of the synthesis of aqueous vanadium pentoxide nematic gels, Langmuir 16 (2000) 5295–5303.
[24] G.T. Chandrappa, N. Steunou, S. Cassaignon, C. Bauvais, P.K. Biswas, J. Livage, Vanadium oxide: from gels to nanotubes, J. Sol-Gel Sci. Technol. 26 (2003) 593–596.
[25] J. Livage, G. Guzman, F. Beteille, P. Davidson, Optical properties of sol-gel derived vanadium oxide films, J. Sol-Gel Sci. Technol. 8 (1997) 857–865.
[26] W. Chen, L. Mai, J. Peng, Q. Xu, Q. Zhu, Raman spectroscopic study of vanadium oxide nanotubes, J. Solid State Chem. 177 (2004) 377–379.
[27] S.H. Lee, H.M. Cheong, M.J. Seong, P. Li, C.E. Tracy, A. Mascarenhas, J.R. Pitts, S.K. Deb., Raman spectroscopic studies of amorphous vanadium oxide thin films, Solid State Ionics 165 (2003) 111–116.
[28] C. Sanchez, J. Livage, G. Lucazeau, Infrared and Raman study of amorphous V_2O_5, J. Raman Spectrosc. 12 (1982) 68–72.
[29] R.J.H. Clark, The Chemistry of Titanium and Vanadium, Elsevier, New York, 1968.
[30] C. Julien, G.A. Nazri, O. Bergstrom, Raman scattering studies of microcrystalline V_6O_{13}, Phys. Status Solidi B 201 (1997) 319–326.
[31] L. Abello, E. Husson, Y. Repelin, G. Lucazeau, Vibrational spectra and valence force field of crystalline V_2O_5, Spectrochim. Acta A39 (1983) 641–651.
[32] I.E. Wachs, J.M. Jehng, F.D. Hardcastle, The interaction of V_2O_5 and Nb_2O_5 with oxide surfaces, Solid State Ionics 32–33 (1989) 904–910.
[33] J.P. Schreckenbach, K. Witke, D. Butte, G. Marx, Characterization of thin metastable vanadium oxide films by Raman spectroscopy, Fresenius J. Anal. Chem. 363 (1999) 211–214.
[34] Y. Zhang, M. Meisel, A. Martin, B. Lücke, K. Witke, K.-W. Brzezinka, In situ Raman investigation on the structural transformation of oxovanadium hydrogenphosphate hemihydrate in the presence of ammonia, Chem. Mater. 9 (1997) 1086–1091.
[35] V.V. Fomichev, P.I. Ukrainskaya, T.M. Ilyin, Vibrational spectra and electrostatic fields of V_2O_5 and lithium vanadium bronzes, Spectrochim. Acta, Part A 53 (1997) 1833–1837.
[36] C.J.T. de Grotthuss, Sur la decomposition de l'eau et des corps qu'elle tient en dissolution a l'aide de l'electricite galvanique, Ann. Chim. 58 (1806) 54–73.
[37] S. Cukierman, Et tu Grotthuss!, Biochim. Biophys. Acta 1757 (2006) 876–878.
[38] N. Agmon, The Grotthuss mechanism, Chem. Phys. Lett. 244 (1995) 456–462.
[39] S. Michailovits, I. Hevesi, P. Liem, Zs. Varfa, Determination of the optical constants and thickness of amorphous V_2O_5 thin films, Thin solid films. Electron. Opt. 102 (1983) 71–76.
[40] A. Gavrilyuk, U. Tritthart, W. Gey, The nature of the photochromism arising in the nanosized MoO3 films, Sol. Energy Mater. Sol. Cells 95 (2011) 1846–1851.
[41] D.L. Dexter, Absorption of light by atoms in solids, Phys. Rev. 101 (1956) 48–55.
[42] A.I. Gavrilyuk, Photochromism in WO_3 thin films, Electrochim. Acta 44 (1999) 3027–3037.